

AD-A 035693

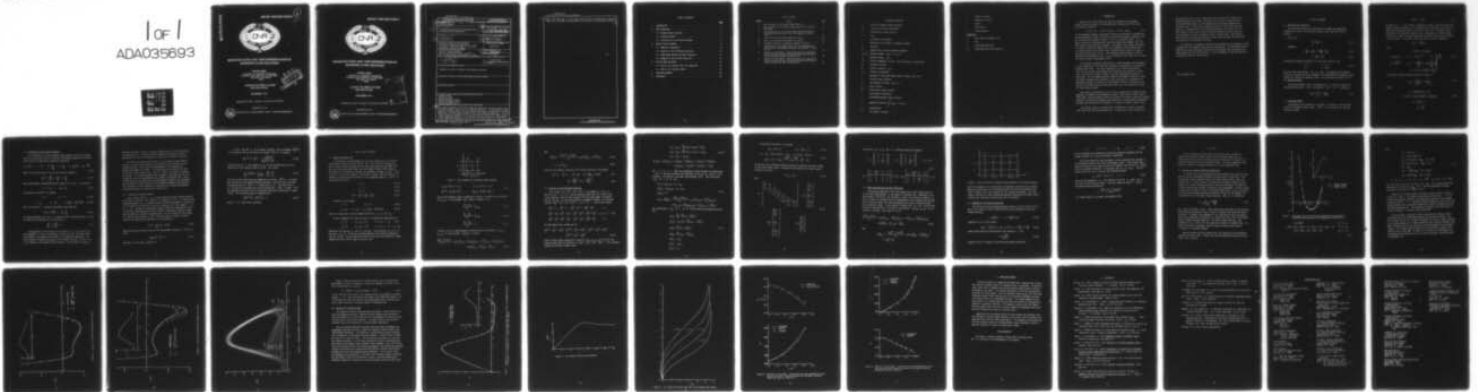
CALIFORNIA STATE UNIV LONG BEACH DEPT OF MECHANICAL --ETC F/G 20/4  
SEPARATED FLOWS AND THEIR REPRESENTATION BY BOUNDARY-LAYER EQUA--ETC(U)  
SEP 76 T CEBCI N00014-75-C-0607

UNCLASSIFIED

ONR-CR215-234-2

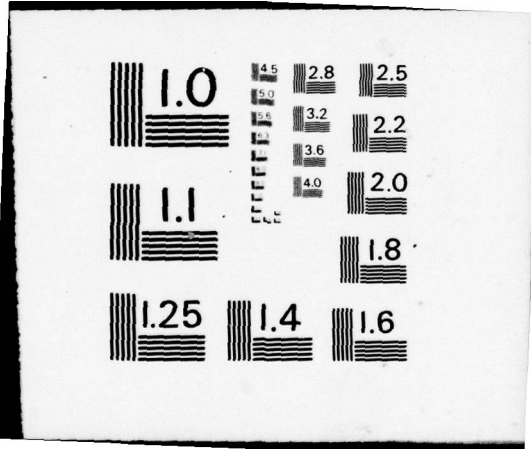
NL

1 of 1  
ADA035693



END

DATE  
FILMED  
3 - 77



ADA 035693

REPORT ONR-CR215-234-2

6



SEPARATED FLOWS AND THEIR REPRESENTATION BY  
BOUNDARY-LAYER EQUATIONS

TUNCER CEBECI  
DEPARTMENT OF MECHANICAL ENGINEERING  
CALIFORNIA STATE UNIVERSITY AT LONG BEACH  
LONG BEACH, CALIFORNIA  
90840

CONTRACT NO. N00014-75-C-0607  
ONR TASK 215-234

SEPTEMBER 1976

DDC  
RECEIVED  
FEB 15 1977  
C

Approved for public release; distribution unlimited.



PREPARED FOR THE  
OFFICE OF NAVAL RESEARCH • 800 N. QUINCY ST. • ARLINGTON • VA • 22217

REPORT ONR-CR215-234-2



SEPARATED FLOWS AND THEIR REPRESENTATION BY  
BOUNDARY-LAYER EQUATIONS

TUNCER CEBECI

DEPARTMENT OF MECHANICAL ENGINEERING  
CALIFORNIA STATE UNIVERSITY AT LONG BEACH  
LONG BEACH, CALIFORNIA  
90840

CONTRACT NO. N00014-75-C-0607  
ONR TASK 215-234

SEPTEMBER 1976

Approved for public release; distribution unlimited.

ACCESSION FOR	Write Section	<input checked="" type="checkbox"/>
NTIS	Buff Section	<input type="checkbox"/>
NO. CONTROL		
IDENTIFICATION		
DISTRIBUTION/AVAILABILITY CODES		
GEN.	AVAIL. AND/OR	SPECIAL

A



PREPARED FOR THE

OFFICE OF NAVAL RESEARCH ● 800 N. QUINCY ST. ● ARLINGTON ● VA ● 22217

UNCLASSIFIED

SECURITY CLASSIFICATION OF THIS PAGE (When Data Entered)

19 REPORT DOCUMENTATION PAGE		READ INSTRUCTIONS BEFORE COMPLETING FORM	
18 1. REPORT NUMBER ONR-CR215-234-2	2. GOVT ACCESSION NO.	3. RECIPIENT'S CATALOG NUMBER	
6 4. TITLE (and Subtitle) SEPARATED FLOWS AND THEIR REPRESENTATION BY BOUNDARY-LAYER EQUATIONS.	9 5. TYPE OF REPORT & PERIOD COVERED Final rept. Jan 1975 - Sept 1976	6. PERFORMING ORG. REPORT NUMBER	
10 7. AUTHOR(s) Tuncer/Cebeci	15 8. CONTRACT OR GRANT NUMBER(s) N00014-75-C-0607	9. PERFORMING ORGANIZATION NAME AND ADDRESS Mechanical Engineering Department California State University at Long Beach Long Beach, California 90840	
11 11. CONTROLLING OFFICE NAME AND ADDRESS Office of Naval Research Vehicle Technology Program - Code 211 800 N. Quincy Street, Arlington, Va. 22217	12. REPORT DATE Sept 1976	10. PROGRAM ELEMENT, PROJECT, TASK AREA & WORK UNIT NUMBERS NR215-234	
12 14. MONITORING AGENCY NAME & ADDRESS (if different from Controlling Office) 12 38p.	13. NUMBER OF PAGES 33	15. SECURITY CLASS. (of this report) Unclassified	
16. DISTRIBUTION STATEMENT (of this Report) Approved for public release; distribution unlimited.			
17. DISTRIBUTION STATEMENT (of the abstract entered in Block 20, if different from Report)			
18. SUPPLEMENTARY NOTES			
19. KEY WORDS (Continue on reverse side if necessary and identify by block number) boundary layers separating flows laminar boundary layers turbulent boundary layers inverse boundary layers			
20. ABSTRACT (Continue on reverse side if necessary and identify by block number) This report presents an efficient numerical method for computing laminar and turbulent boundary layers with and without separation. It represents a major extension to the earlier work described by the author and makes use of Keller's two-point finite-difference method to solve the governing equations. The non-linear eigenvalue approach of the earlier work was found to be inappropriate to the separating boundary layers which are the main concern of this report and an alternative-approach, based on the solution procedures of Cebeci and			

UNCLASSIFIED

SECURITY CLASSIFICATION OF THIS PAGE (When Data Entered)

cont.

Keller has been used. The solutions, which relate to attached and separating flows, were obtained with prescribed distributions of displacement thickness.

UNCLASSIFIED

SECURITY CLASSIFICATION OF THIS PAGE (When Data Entered)

## TABLE OF CONTENTS

	<u>Page</u>
1. INTRODUCTION . . . . .	1
2. BASIC EQUATIONS . . . . .	3
2.1 Boundary-Layer Equations . . . . .	3
2.2 Turbulence Model . . . . .	3
2.3 Formulation of the Inverse Problems . . . . .	5
3. Mechul Function Method . . . . .	8
3.1 Numerical Formulation . . . . .	8
3.2 Solution of the Difference Equations . . . . .	10
3.3 FLARE Approximation and DUIT Procedures . . . . .	13
3.4 Comments on the Solution Algorithm . . . . .	14
4. RESULTS AND DISCUSSION . . . . .	16
4.1 Results for Laminar Flows with Separation . . . . .	16
4.2 Results for Turbulent Flows . . . . .	22
5. CONCLUDING REMARKS . . . . .	28
6. REFERENCES . . . . .	29

LIST OF FIGURES

<u>Figure</u>	<u>Title</u>	<u>Page</u>
1	Net rectangle for difference approximations . . . . .	9
2	Net rectangle for difference approximations for the DUIT procedure . . . . .	14
3	Calculated local skin-friction coefficient distribution for separating and reattaching flow computed by Briley (1971). . . . .	17
4	Local skin-friction distribution for Case A . . . . .	19
5	Local skin-friction distribution for Case B . . . . .	20
6	Streamline pattern in separation bubble for Case B . . . . .	21
7	Comparison of calculated results for the separated flow for which the displacement-thickness distribution is given by 4.4. . . . .	23
8	Results for flow 4400. (Inverse results were obtained by using both the nonlinear eigenvalue method and the Mechul- function method and they are identical.) . . . . .	26
9	Results for flow 4800. (Inverse results were obtained by using both the nonlinear eigenvalue method and the Mechul- function method and they are identical.) . . . . .	27

## PRINCIPAL NOTATION

A	Van Driest damping length parameter
$c_f$	local skin-friction coefficient
f	dimensionless stream function
$f'$	$u/u_e$
K	variable grid parameter
L	modified mixing length, or reference length
p	pressure
$p^+$	dimensionless pressure-gradient parameter
$R_x, R_L$	Reynolds number, $u_e x/\nu$ or $u_e L/\nu$
$R_\theta$	Reynolds number, $u_e \theta/\nu$
u, v	velocity components in the x- and y-directions, respectively
$u_0$	reference velocity
$u_\tau$	friction velocity ( $\tau_w/\rho$ )
x, y	Cartesian coordinates
$\alpha$	parameter in the outer eddy-viscosity formula, see (2.8)
$\delta$	boundary-layer thickness
$\delta^*$	displacement thickness, see (2.5)
$\epsilon_m$	eddy viscosity
$\epsilon_m^+$	dimensionless eddy viscosity
$\eta$	transformed y-coordinate
$\eta_\infty$	transformed boundary-layer thickness
$\theta$	momentum thickness, $\int_0^\infty u/u_e (1 - u/u_e) dv$
$\gamma_{tr}$	intermittency
$\kappa$	Von Karman's constant

$\mu$  dynamic viscosity  
 $\nu$  kinematic viscosity  
 $\rho$  density  
 $\tau$  shear stress  
 $\psi$  stream function

Subscripts

e outer edge of boundary layer  
w wall  
 $\infty$  freestream conditions  
( )' differentiation with respect to  $n$

## 1. INTRODUCTION

Boundary-layer calculations are usually performed for prescribed boundary conditions which, for two-dimensional incompressible flows, may be provided in the form

$$u(x,0) = 0, \quad v(x,0) = v_w(x), \quad u(x,\delta) = u_e(x) \quad (1.1)$$

In some problems, however, the external velocity distribution is unknown and can be determined in order to satisfy an alternative boundary condition, such as prescribed displacement thickness,  $\delta^*(x)$ , or the wall shear,  $\tau_w(x)$ . These solutions are obtained with "inverse boundary-layer methods" and find application in many practical problems. For example, the airfoils discussed in a recent article by Liebeck (1976) are designed on the principle that, in certain regions of an airfoil flow, the deceleration results in values of wall shear stress close to zero. Other important applications of inverse boundary-layer procedures occur in the calculation of duct flows such as those discussed by Cebeci and Bradshaw (1977).

A particularly important application of inverse boundary-layer procedures is their potential to calculate the properties of separating and reattaching boundary-layer flows. It is well known that, for a prescribed external velocity distribution, the boundary-layer equations are singular at separation: they are not singular, however, when the displacement thickness is prescribed. This was demonstrated by Catherall and Mangler (1966) who solved the laminar boundary-layer equations in the usual way until separation was approached and then, by assuming a displacement-thickness distribution, calculated the external-velocity distribution and local flow properties through the recirculation region.

More recent investigations of the inverse boundary-layer method have been reported, for example, by Klineberg and Steger (1974), Horton (1974), Carter (1974,1975), Carter and Wornom (1975) and Williams (1975,1976), and have involved solutions to the laminar boundary-layer equations with prescribed displacement-thickness and shear-stress distributions in regions of negative shear stress.

The present report is concerned with incompressible turbulent boundary-layer flows with and without separation. It represents a major extension to

the work described by Cebeci (1975a), which was concerned with compressible, attached boundary-layer flows, and makes use of Keller's (1970) two-point finite-difference method to solve boundary-layer equations appropriate to turbulent flow. The nonlinear eigenvalue approach of the earlier work was found to be inappropriate to the separating boundary layers which are the main concern of this report and an alternative-approach, based on the solution procedures of Cebeci and Keller (1972), has been used. The solutions, which relate to attached and separating flows, were obtained with prescribed distributions of displacement thickness.

The equations and boundary conditions are presented in the following section together with the algebraic eddy-viscosity formulation. The succeeding sections describe the solution method, referred to as the Mechul\*-function method, and these results and their implications. A brief statement of the more important conclusions forms the final section.

\*lit. unknown (Turk.)

## 2. BASIC EQUATIONS

### 2.1 Boundary-Layer Equations

The conservation equations appropriate for steady two-dimensional incompressible laminar and turbulent boundary layers may be written as follows:

Continuity:

$$\frac{\partial u}{\partial x} + \frac{\partial v}{\partial y} = 0 \quad (2.1)$$

Momentum:

$$u \frac{\partial u}{\partial x} + v \frac{\partial u}{\partial y} = -\frac{1}{\rho} \frac{dp}{dx} + \frac{1}{\rho} \frac{\partial \tau}{\partial y} \quad (2.2)$$

$$\tau = \mu \frac{\partial u}{\partial y} - \rho \overline{u'v'} \quad (2.3)$$

Corresponding boundary conditions, for zero mass transfer, are:

$$\begin{array}{ll} y = 0 & u, v = 0 \\ y \rightarrow \infty & u \rightarrow u_e(x) \end{array} \quad (2.4)$$

With specified distributions  $p(x)$  or  $u_e(x)$ , the equations and boundary conditions represent the usual statement of the two-dimensional boundary-layer problem for laminar and turbulent flows. For convenience, we shall call it the standard problem.

The inverse problem, which we consider here, is a flow with specified displacement thickness,  $\delta^*(x)$ , distribution. Here  $\delta^*(x)$  is defined by

$$\delta^*(x) = \int_0^{\infty} \left(1 - \frac{u}{u_e}\right) dy \quad (2.5)$$

### 2.2 Turbulence Model

The solution of the equations in section 2.1 requires a closure assumption for the Reynolds shear stress,  $-\rho \overline{u'v'}$ . In our study we use the eddy-viscosity concept

$$-\overline{\rho u'v'} = \rho \epsilon_m \frac{\partial u}{\partial y} \quad (2.6)$$

and prescribe  $\epsilon_m$  in the manner recommended by Cebeci and Smith (1974) and shown by them to represent various boundary-layer conditions such as those at high- and low-Reynolds numbers, transition flows, etc. According to this formulation, the turbulent boundary layer is regarded as a composite layer consisting of inner and outer regions with different eddy-viscosity formulas for each region. In the inner region the eddy viscosity is defined by

$$(\epsilon_m)_i = L^2 \frac{\partial u}{\partial y} \gamma_{tr}$$

where

$$L = 0.4y[1 - \exp(-y/A)]$$

$$A = 26 \frac{\nu}{N} u_\tau^{-1}, \quad N = (1 - 11.8p^+)^{1/2}, \quad p^+ = \frac{\nu u_e}{3} \frac{du_e}{dx} \quad (2.7)$$

$$u_\tau = \left(\frac{\tau_w}{\rho}\right)^{1/2}, \quad \gamma_{tr} = 1 - \exp\left[-G(x - x_{tr}) \int_{x_{tr}}^x \frac{dx}{u_e}\right]$$

$$G = 8.35 \times 10^{-4} (u_e^3/\nu^2) R_{x_{tr}}^{-1.34}$$

In the outer region the eddy viscosity is given by

$$(\epsilon_m)_o = \alpha \left| \int_0^\infty (u_e - u) dy \right| \gamma_{tr} \quad (2.8)$$

where

$$\alpha = 0.0168[1.55/(1 + \Pi)]$$

$$\Pi = 0.55[1 - \exp(-0.243z_1^{1/2} - 0.298z_1)] \quad (2.9)$$

$$z_1 = R_\theta/425 - 1$$

$$R_\theta = \frac{u_e \nu}{\nu}$$

### 2.3 Formulation of the Inverse Problems

In our approach to inverse boundary-layer problems, we use the stream function concept and write the continuity and momentum equations as a third-order system in dimensionless quantities defined by

$$\bar{y} = \frac{y}{L} \sqrt{R_L}, \quad \bar{x} = \frac{x}{L}, \quad \bar{p} = \frac{p}{\rho u_0^2}, \quad \bar{u} = \frac{u}{u_0}, \quad \bar{v} = \frac{v}{u_0} \sqrt{R_L}, \quad R_L = \frac{u_0 L}{\nu} \quad (2.10)$$

Then it can be shown that (2.1) and (2.2) can be written as

$$(b\psi'')' - \frac{d\bar{p}}{d\bar{x}} = \psi' \frac{\partial \psi'}{\partial \bar{x}} - \psi'' \frac{\partial \psi}{\partial \bar{x}} \quad (2.11)$$

Here primes denote differentiation with respect to  $\bar{y}$  and  $b$  is given by:

$$b = 1 + \epsilon_m^+, \quad \epsilon_m^+ = \epsilon_m / \nu \quad (2.12)$$

The boundary conditions (2.5) become

$$\bar{y} = 0 \quad \psi = \psi' = 0 \quad (2.13a)$$

$$\bar{y} = y_e \quad \psi' = \bar{u}_e, \quad \psi = \bar{u}_e [\bar{y}_e - \sqrt{R_L} \bar{\delta}^*(x)] \quad (2.13b)$$

where the subscript  $e$  denotes the boundary-layer edge and

$$\bar{\delta}^*(x) = \frac{\delta^*(x)}{L}, \quad \bar{u}_e = \frac{u_e}{u_0} \quad (2.14)$$

The relation between  $\bar{u}_e$  and  $\bar{p}$  is given by Euler's equation which, in terms of dimensionless quantities, can be written as

$$\frac{d\bar{p}}{d\bar{x}} + \bar{u}_e \frac{d\bar{u}_e}{d\bar{x}} = 0 \quad (2.15)$$

Two approaches to the solution of the system (2.11), (2.13) and (2.15) were attempted. In the first approach, which we call the "nonlinear eigenvalue method," the pressure was treated, as an eigenvalue parameter. The second approach regarded the pressure as an unknown function; we shall refer to this method as the "Mechul-function method." The nonlinear eigenvalue

method is described in detail in Cebeci (1975a) and only a brief description is presented here. The Mechul-function method, which proved to be more appropriate to flows with separation, is described in detail in section 3.

For flows with negative wall shear, it is necessary to make approximations to the governing equations to continue the calculations past the separation point. Here we use the approximation first suggested by Reyhner and Flügge-Lotz (1968). This approximation referred to as FLARE by Williams (1975), neglects the  $u(\partial u/\partial x)$  term in the region of negative  $u$ -velocity. All inverse boundary-layer procedures, including the ones described here, use this approximation for regions of separated flow. Once a solution has been obtained with this approximation, however, the assumption can be relaxed to allow solutions of the complete boundary-layer equations. This relaxation of the assumption is effected with a forward and backward difference procedure, as described in section 3.3.

### 2.3.1 Nonlinear Eigenvalue Method

Let us assume that at  $x = x_0$  we are given the initial velocity profiles and we seek a solution of the system (2.11) subject to (2.13). In the nonlinear eigenvalue method,  $\bar{u}_e$  is assumed and with (2.15) we then obtain a solution of (2.11) subject to (2.13a) and to the first relation in (2.13b), namely  $\psi' = \bar{u}_e$  at  $y = y_e$ . Solutions were obtained by Cebeci (1975a) for compressible flows, in which the governing equations were solved in transformed variables rather than the physical variables considered here. For the solution we can compute  $\bar{\delta}^*$  (which we shall denote by  $\bar{\delta}_c^*$ ) from (2.5) which, in terms of stream function and dimensionless quantities, can be written as

$$\bar{\delta}_c(x) = \frac{1}{\sqrt{R_L}} (y_e - \psi_e/\bar{u}_e) \quad (2.16)$$

Recalling that the desired value for the displacement thickness is  $\bar{\delta}^*(x)$ , we form:

$$\phi[\bar{u}_e(x)] \equiv \bar{\delta}_c^* - \bar{\delta}^* \quad (2.17)$$

and seek  $\bar{u}_e$  such that  $\phi[\bar{u}_e(x)] \equiv 0$ .

To solve  $\phi[\bar{u}_e(x)] = 0$ , we use Newton's method. With an estimate  $\bar{u}_e^{(0)}(x)$  of the external velocity we define the sequence  $\bar{u}_e^{(v)}(x)$  by setting

$$\bar{u}_e^{(v+1)}(x) = \bar{u}_e^{(v)} - \frac{\phi[u_e^v(x)]}{\partial\phi[u_e^v(x)] / \partial\bar{u}_e} \quad (2.18)$$

The derivative of  $\phi$  with respect to  $\bar{u}_e$  can be obtained from (2.17) by making use of the relation given by (2.16). This gives

$$\frac{\partial}{\partial\bar{u}_e} \phi[u_e^v(x)] = \frac{1}{\bar{u}_e \sqrt{R_L}} - \frac{\partial\psi_e}{\partial\bar{u}_e} + \frac{\psi_e}{\bar{u}_e} \quad (2.19)$$

One step of the iteration may be summarized as follows:  $u_e^{(0)}(x)$  is assumed and a solution of the standard problem obtained. From this result and from the desired value of  $\bar{\delta}^*(x)$ ,  $\phi$  is found from (2.17). The next value of  $\bar{u}_e$  can then be calculated from (2.18) provided that  $\partial\phi/\partial\bar{u}_e$  is known. That is, obtained by solving a set of variational equations as described in Cebeci (1976). The iteration process is repeated until

$$\left| \bar{u}_e^{(v+1)}(x) - \bar{u}_e^{(v)}(x) \right| < \delta_1 \quad (2.20)$$

where  $\delta_1$  is a small error tolerance.

### 3. MECHUL FUNCTION METHOD

#### 3.1 Numerical Formulation

In the Mechul function method, we solve the system (2.11), (2.13) with the numerical method of Keller (1970). This is an efficient accurate two-point finite-difference method that has been used extensively by Cebeci for two- and three-dimensional flows (see, for example, Cebeci (1974, 1975b)). According to this method we introduce new dependent variables  $u(\bar{x}, \bar{y})$ ,  $v(\bar{x}, \bar{y})$  so that (2.11) can be written as a first-order system. With the function  $\bar{p}$  treated as unknown and with the help of the y-momentum equation ( $-\partial\bar{p}/\partial\bar{y} = 0$ ) we can write (2.11) as

$$\psi' = u \quad (3.1a)$$

$$u' = v \quad (3.1b)$$

$$p' = 0 \quad (3.1c)$$

$$(bv)' - \frac{\partial p}{\partial x} = u \frac{\partial u}{\partial x} - v \frac{\partial \psi}{\partial x} \quad (3.1d)$$

Similarly (2.13) becomes

$$y = 0 \quad \psi = u = 0 \quad (3.2a)$$

$$y = y_e; \quad u = u_e, \quad \psi_e = u_e [y_e - \sqrt{R_L} \delta^*(x)] \quad (3.2b)$$

Here, for convenience, we have dropped the bars on  $x$ ,  $y$ ,  $p$  and  $u_e$ .

On the rectangular net shown in figure 1, we denote the node points by

$$x_0 = 0, \quad x_n = x_{n-1} + k_n \quad n = 1, 2, \dots, N \quad (3.3)$$

$$y_0 = 0, \quad y_j = y_{j-1} + h_j \quad j = 1, 2, \dots, J : y_J = y_e$$

Nonuniform net spacings  $k_n$  and  $h_j$  are used. The quantities  $(\psi, u, v, p)$  at points  $(x_n, y_j)$  of the net are approximated by net functions denoted by  $(\psi_j^n, u_j^n, v_j^n, p_j^n)$ . We also employ the notation for points and quantities midway between net points and for any net function  $q_j^n$ :

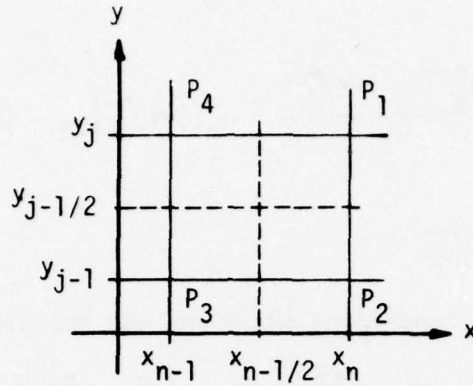


Figure 1. Net rectangle for difference approximations.

$$\begin{aligned}
 x_{n-1/2} &\equiv \frac{1}{2} (x_n + x_{n-1}) & , & & n_{j-1/2} &\equiv \frac{1}{2} (n_j + n_{j-1}) \\
 q_j^{n-1/2} &\equiv \frac{1}{2} (q_j^n + q_j^{n-1}) & , & & q_{j-1/2}^n &\equiv \frac{1}{2} (q_j^n + q_{j-1}^n)
 \end{aligned} \tag{3.4}$$

The finite-difference forms of equations (3.1a,b,c), written for the midpoint  $(x^n, y_{j-1/2})$  of the segment  $P_1P_2$  shown in figure 1, are

$$\frac{\psi_j^n - \psi_{j-1}^n}{h_j} = u_{j-1/2}^n \tag{3.5a}$$

$$\frac{u_j^n - u_{j-1}^n}{h_j} = v_{j-1/2}^n \tag{3.5b}$$

$$\frac{p_j^n - p_{j-1}^n}{h_j} = 0 \tag{3.5c}$$

Similarly (3.1d) is approximated by centering about the midpoint  $(x_{n-1/2}, y_{j-1/2})$  of the rectangle  $P_1P_2P_3P_4$  to obtain

$$\begin{aligned}
 \frac{b_j^n v_j^n - b_{j-1}^n v_{j-1}^n}{h_j} + \alpha_n [(\psi v)_{j-1/2}^n + v_{j-1/2}^{n-1} \psi_{j-1/2}^n - (u^2)_{j-1/2}^n - \psi_{j-1/2}^{n-1} v_{j-1/2}^n] \\
 - 2\alpha_n [p_{j-1/2}^n - p_{j-1/2}^{n-1}] = R_{j-1/2}^{n-1}
 \end{aligned} \tag{3.5d}$$

Here

$$R_{j-1/2}^{n-1} = -\frac{(bv)_j^{n-1} - (bv)_{j-1}^{n-1}}{h_j} + \alpha_n [(\psi v)_{j-1/2}^{n-1} - (u^2)_{j-1/2}^{n-1}] \quad (3.6a)$$

$$\alpha_n = \frac{1}{x_n - x_{n-1}} \quad (3.6b)$$

Similarly the boundary conditions (3.2) and the relation (2.15) become

$$\psi_0^n = 0, \quad u_0^n = 0, \quad u_J^n = u_e^n, \quad \psi_J^n = u_e^n [y_e - \bar{\delta}^*(x)] \quad (3.7)$$

$$p^n + \frac{(u_e^2)^n}{2} = p^{n-1} + \frac{(u_e^2)^{n-1}}{2} \quad (3.8)$$

### 3.2 Solution of the Difference Equations

If we assume  $(\psi_j^{n-1}, u_j^{n-1}, v_j^{n-1}, p_j^{n-1})$  to be known for  $0 \leq j \leq J$ , then (3.5) for  $1 \leq j \leq J-1$  and the boundary conditions (3.7) yield a non-linear algebraic system of  $4J+4$  equations with the same number of unknowns  $(\psi_j^n, u_j^n, v_j^n, p_j^n)$ . To solve the system we use Newton's method. We introduce iterates  $[\psi_j^{(v)}, u_j^{(v)}, v_j^{(v)}, p_j^{(v)}]$   $v = 0, 1, 2, \dots$ , with initial values

$$\begin{aligned} \psi_0^{(0)} &= 0, \quad u_0^{(0)} = 0, \quad v_0^{(0)} = v_0^{n-1}, \quad p_0^{(0)} = p_0^{n-1} & j = 0 \\ \psi_j^{(0)} &= \psi_j^{n-1}, \quad u_j^{(0)} = u_j^{n-1}, \quad v_j^{(0)} = v_j^{n-1}, \quad p_j^{(0)} = p_j^{n-1} & 1 \leq j \leq J-1 \\ \psi_J^{(0)} &= \psi_J^{n-1}, \quad u_J^{(0)} = u_e^{n-1}, \quad v_J^{(0)} = v_J^{n-1}, \quad p_J^{(0)} = p_J^{n-1} & j = J \end{aligned} \quad (3.9)$$

For the higher-order iterates we set

$$\begin{aligned} \psi_j^{(v+1)} &= \psi_j^{(v)} + \delta\psi_j^{(v)}, \quad u_j^{(v+1)} = u_j^{(v)} + \delta u_j^{(v)}, \quad v_j^{(v+1)} = v_j^{(v)} + \delta v_j^{(v)} \\ p_j^{(v+1)} &= p_j^{(v)} + \delta p_j^{(v)} \end{aligned} \quad (3.10)$$

Then we insert these expressions in place of  $[\psi_j, u_j, v_j, p_j]$  in (3.5) and drop the terms that are quadratic in  $[\delta\psi_j^{(v)}, \delta u_j^{(v)}, \delta v_j^{(v)}, \delta p_j^{(v)}]$ . This procedure yields the following linear system:

$$\begin{aligned}
\delta\psi_j - \delta\psi_{j-1} - \frac{h_j}{2} (\delta u_j + \delta u_{j-1}) &= (r_1)_j \\
\delta u_j - \delta u_{j-1} - \frac{h_j}{2} (\delta v_j + \delta v_{j-1}) &= (r_3)_{j-1} \\
\delta P_j - \delta P_{j-1} &= (r_4)_{j-1}
\end{aligned} \tag{3.11}$$

$$\begin{aligned}
(s_1)_j \delta v_j + (s_2)_j \delta v_{j-1} + (s_3)_j \delta \psi_j + (s_4)_j \delta \psi_{j-1} + (s_5)_j \delta u_j + (s_6)_j \delta u_{j-1} \\
+ (s_7)_j \delta P_j + (s_7)_{j-1} \delta P_{j-1} = (r_2)_j
\end{aligned}$$

for  $j = 1, 2, \dots, J$ . Here for convenience we have dropped the superscripts  $v$  and  $n$ , and have reordered the equations so that the  $A_0$  matrix is not singular. (For details, see Cebeci and Bradshaw, 1977.) The coefficients  $(r_k)_j$  ( $k = 1$  to  $4$ ) are:

$$\begin{aligned}
(r_1)_j &= h_j u_{j-1/2} - \psi_j + \psi_{j-1} \\
(r_3)_{j-1} &= h_j v_{j-1/2} - u_j + u_{j-1} \\
(r_4)_{j-1} &= 0
\end{aligned} \tag{3.12}$$

$$\begin{aligned}
(r_2)_j &= R_{j-1/2}^{n-1} - \frac{(bv)_j - (bv)_{j-1}}{h_j} + \alpha_n [(\psi v)_{j-1/2} + v_{j-1/2}^{n-1} \psi_{j-1/2} - \\
&\quad - (u^2)_{j-1/2} - \psi_{j-1/2}^{n-1} v_{j-1/2}] - 2\alpha_n (P_{j-1/2} - P_{j-1/2}^{n-1})
\end{aligned}$$

The coefficients  $(s_k)_j$  ( $k = 1$  to  $7$ ) of the differenced momentum equation are:

$$\begin{aligned}
(s_1)_j &= \frac{b_j}{h_j} + \frac{\alpha_n}{2} (\psi_j - \psi_{j-1/2}^{n-1}) \\
(s_2)_j &= -b_{j-1}/h_j + \frac{\alpha_n}{2} (\psi_{j-1} - \psi_{j-1/2}^{n-1}) \\
(s_3)_j &= \frac{\alpha_n}{2} (v_j + v_{j-1/2}^{n-1}) \\
(s_4)_j &= \frac{\alpha_n}{2} (v_{j-1} + v_{j-1/2}^{n-1}) \\
(s_5)_j &= -\alpha_n u_j \\
(s_6)_j &= -\alpha_n u_{j-1} \\
(s_7)_j &= -\alpha_n
\end{aligned} \tag{3.13}$$



The matrices  $A_j, B_j, C_j$  are  $4 \times 4$  matrices which are given by

$$\begin{aligned}
 A_0 &\equiv \begin{bmatrix} 1 & 0 & 0 & 0 \\ 0 & 1 & 0 & 0 \\ 0 & -1 & -h_0/2 & 0 \\ 0 & 0 & 0 & 1 \end{bmatrix} & C_j &\equiv \begin{bmatrix} 0 & 0 & 0 & 0 \\ 0 & 0 & 0 & 0 \\ 0 & 1 & -h_0/2 & 0 \\ 0 & 0 & 0 & 1 \end{bmatrix} & 0 \leq j \leq J-1 \\
 B_j &= \begin{bmatrix} -1 & -h_j/2 & 0 & 0 \\ (s_4)_j & (s_6)_j & (s_2)_j & (s_7)_j \\ 0 & 0 & 0 & 0 \\ 0 & 0 & 0 & 0 \end{bmatrix} & 1 \leq j \leq J; & A_j &= \begin{bmatrix} 1 & -h_j/2 & 0 & 0 \\ (s_3)_j & (s_5)_j & (s_1)_j & (s_7)_j \\ 0 & -1 & -h_j/2 & 0 \\ 0 & 0 & 0 & -1 \end{bmatrix} & 1 \leq j \leq J
 \end{aligned} \tag{3.17}$$

### 3.3 FLARE Approximation and DUIT Procedures

As previously mentioned, flows with negative wall shear require the use of the FLARE approximation in the region of reversed flow. According to this approximation,  $u_j^n$  and  $u_j^{n-1}$  are set equal to zero in the region of negative  $u_j$ . Once a solution is obtained with this approximation, more accurate calculations can be obtained without the FLARE approximation by using a forward and backward difference scheme. In the region of reverse flow ( $u_j \leq 0$ ), we write the difference approximations of (3.1d) for the midpoint  $(x_{n+1/2}, y_{j-1/2})$  of the rectangle  $P_1P_2P_3P_4$  (see figure 2) to get

$$\begin{aligned}
 \frac{(bv)_j^n - (bv)_{j-1}^n}{h_j} - \beta[(\psi v)_{j-1/2}^n + v_{j-1/2}^{n+1} \psi_{j-1/2}^n - (u^2)_{j-1/2}^n - \psi_{j-1/2}^{n+1} v_{j-1/2}^n] \\
 - 2\beta[P_{j-1/2}^{n+1} - P_{j-1/2}^n] = R_{j-1/2}^{n+1}
 \end{aligned} \tag{3.18}$$

Here

$$\begin{aligned}
 R_{j-1/2}^{n+1} &= -\frac{(bv)_j^{n+1} - (bv)_{j-1}^{n+1}}{h_j} + \beta[(\psi v)_{j-1/2}^{n+1} + (u^2)_{j-1/2}^{n+1}] \\
 \beta &= \frac{1}{x_{n+1} - x_n}
 \end{aligned}$$

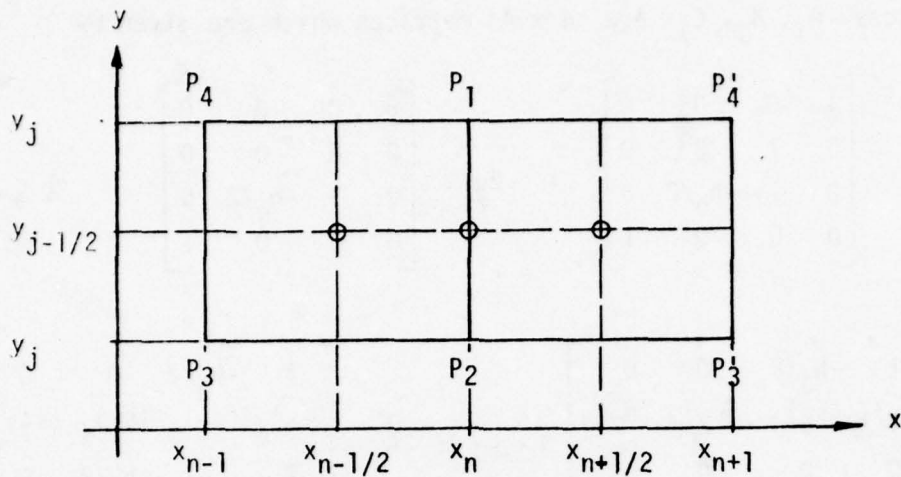


Figure 2. Net rectangle for difference approximations for the DUIT procedure.

With this procedure, the calculations are repeated, starting at the x-station where the calculations first indicated reverse flow and are continued to the final x-station, until the solutions do not indicate any changes. This procedure, referred to as DUIT (downstream upstream iteration) by Williams (1975), usually gives converged solutions with two or three DUITs.

### 3.4 Comments on the Solution Algorithm

The solution of the governing equations given by (2.1) to (2.4) or (2.11) and (2.13), requires initial conditions which can be obtained in the transformed variables,

$$\eta = \sqrt{u_e/\nu x} y \quad , \quad \psi = \sqrt{u_e \nu x} f(x, \eta) \quad (3.20)$$

Equations (2.1) to (2.4) become:

$$(bf'')' + \frac{m+1}{2} ff'' + m[1 - (f')^2] = x f' \frac{\partial f'}{\partial x} - f'' \frac{\partial f}{\partial x} \quad (3.21)$$

where primes indicate differentiation with respect to  $\eta$  and

$$m = \frac{x}{u_e} \frac{du_e}{dx} \quad (3.22)$$

Equation (3.21) is subject to the following boundary conditions:

$$\eta = 0 \quad f = f' = 0 \quad \eta \rightarrow \eta_{\infty} \quad f' \rightarrow 1 \quad (3.23)$$

Initial conditions were obtained by solving the governing equations for the standard problem to a location upstream of separation.

The present method has been developed to allow nonuniform net spacings in the streamwise direction and across the boundary layer. In the latter case, a geometric progression has been used with the property that the ratio of lengths of any two adjacent intervals is a constant; that is,  $h_j = Kh_{j-1}$ . The distance to the  $j$ -th line is given by the following formula:

$$\eta_j = h_1 (K^j - 1) / (K - 1) \quad K > 1 \quad (3.24)$$

There are two parameters:  $h_1$ , the length of the first  $\Delta\eta$  step, and  $K$ , the ratio of two successive steps. The total number of points  $J$  can be calculated from the expression,

$$J = \frac{\ln[1 + (K - 1)(\eta_{\infty}/h_1)]}{\ln K} \quad (3.25)$$

For further details, see Cebeci and Bradshaw (1977).

## 4. RESULTS

To test the Mechul function method calculations were performed for laminar and turbulent boundary layers with and without separation, and compared with the results of previous numerical solutions for laminar flows and with experimental data for turbulent flows. The latter comparisons were made for a number of attached flows and only for one separated flow.

### 4.1 Results for Laminar Flows with Separation

For laminar flows with separation we have considered four separate flows which allow the displacement thickness distribution to be specified. These include the laminar separated flows of Williams (1976), Carter (1975) and Briley (1971). In the last case, the free-stream boundary condition corresponded to a linearly decreasing external velocity distribution followed by a constant velocity and resulted in separation and reattachment. Figure 3 allows a comparison of values of local skin-friction coefficient  $c_f \sqrt{R_L}$  calculated with the present method with those obtained by Briley from the steady, two-dimensional form of the Navier-Stokes equations. Here  $c_f$  is defined by

$$c_f = \frac{\tau_w}{1/2 \rho u_0^2} = \frac{2\psi''(0)}{\sqrt{R_L}} \quad (4.1)$$

and  $c_f \sqrt{R_L}$  represents  $2\psi''(0)$ . These calculations were made for the displacement thickness distribution (see in figure 3) deduced from the Navier-Stokes solutions. In general, the agreement is very good and the small discrepancy may be associated with the difficulty of reading the input  $\bar{\delta}^*(x)$  distribution from the graph presented by Briley. The Navier-Stokes solutions were obtained for  $R_L = 2.08 \times 10^4$  and required 45 minutes on a UNIVAC 1108. The results obtained by the Mechul function approach required approximately 10 seconds on a CDC-6600 computer.

We next consider the two laminar flows with separation and reattachment computed by Carter (1975). These flows have displacement-thickness distributions  $\delta^*(x)$  given by

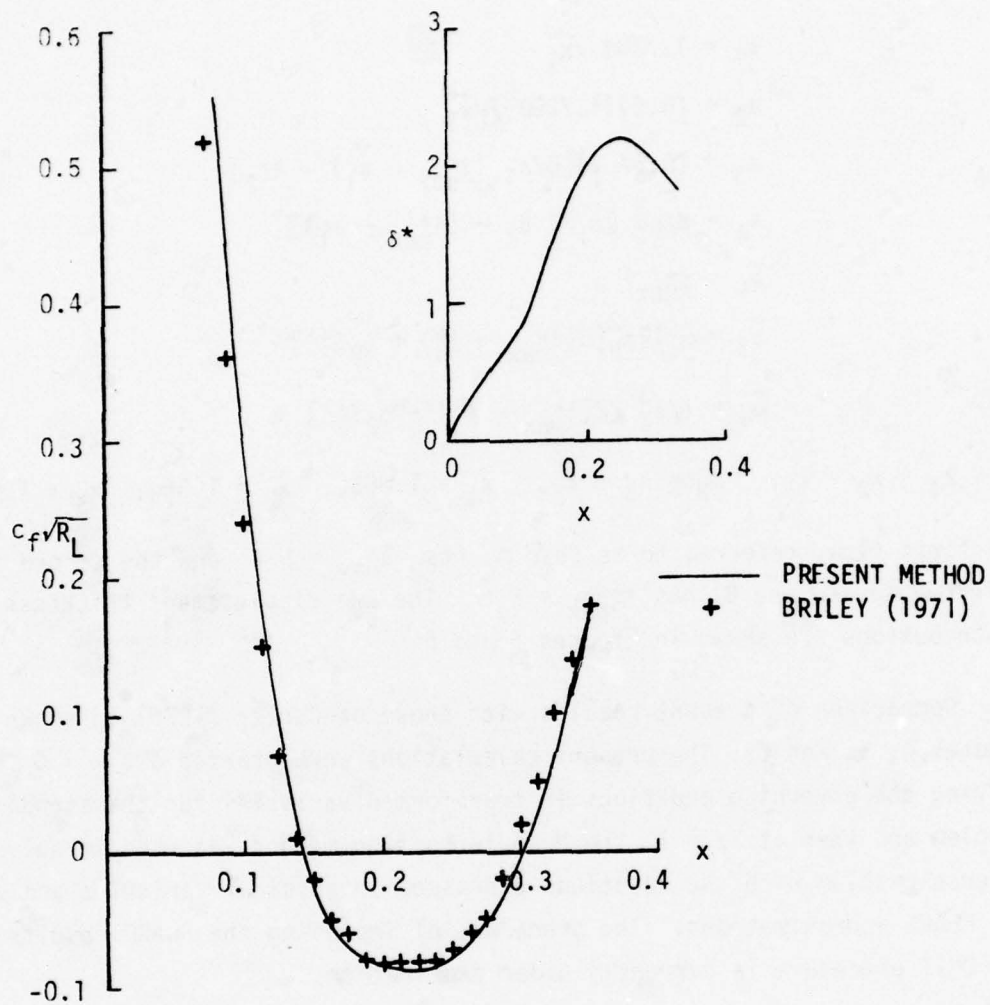


Figure 3. Calculated local skin-friction coefficient distribution for separating and reattaching flow computed by Briley (1971).

$$\bar{\delta}^*(x) \equiv \begin{cases} 1.7208\sqrt{x} & 1.0 \leq x \leq x_1 \\ a_1 + a_2(x - x_1) + a_3(x - x_1)^2 + a_4(x - x_1)^3 & x_1 \leq x \leq x_2 \\ \bar{a}_1 + \bar{a}_3(x - x_2)^2 + \bar{a}_4(x - x_2)^3 & x_2 \leq x \leq x_3 \end{cases} \quad (4.2)$$

with

$$\begin{aligned}
 a_1 &= 1.7208 \sqrt{x_1} \\
 a_2 &= (0.5)(1.7208)/\sqrt{x_1} \\
 a_3 &= (0.5/\Delta_1)[6/\Delta_1 (\delta_{\max}^* - a_1) - 4a_2] \\
 a_4 &= 2/\Delta_1^3 [\Delta_1/2 a_2 - (\delta_{\max}^* - a_1)] \\
 \bar{a}_1 &= \delta_{\max}^* \\
 \bar{a}_3 &= -1/\Delta_2^2 [3(\delta_{\max}^* - \delta_3^*) + \Delta_2 \delta_3^{*'}] \\
 \bar{a}_4 &= 1/\Delta_2^3 [2(\delta_{\max}^* - \delta_3^*) + \Delta_2 \delta_3^{*'}]
 \end{aligned} \tag{4.3}$$

$$\Delta_1 = x_2 - x_1, \quad \Delta_2 = x_3 - x_2, \quad x_1 = 1.065, \quad x_2 = 1.35, \quad x_3 = 1.884$$

The first flow, referred to as Case A, has  $\delta_{\max}^* = 5.6$ , and the second flow referred to as Case B, has  $\delta_{\max}^* = 8.6$ . The two displacement thickness distributions are shown in Figures 5 and 6.

Comparison of present results with those of Carter (1975) is shown in Figures 4, 5, and 6. The present calculations were started at  $x = 0$  by solving the governing equations in transformed variables for the standard problem and then at  $x = 1$  the Mechul-function method was used to solve the inverse problem with the equations expressed in physical variables and with the FLARE approximations. The procedure of improving the FLARE results by the DUIT procedure is currently under examination.

As can be seen, the present results agree well with those of Carter which made use of the FLARE approximations and the DUIT procedure. Our skin-friction results are in better agreement with Carter's results obtained by the FLARE procedure. His FLARE approximation was slightly different from that considered here and may account for the disagreement with the present results. The computer time associated with the results was again of the order of 10s on a CDC 6600. At almost all  $x$ -stations the convergence rate was quadratic and required only two or three iterations, including regions of separated flow.

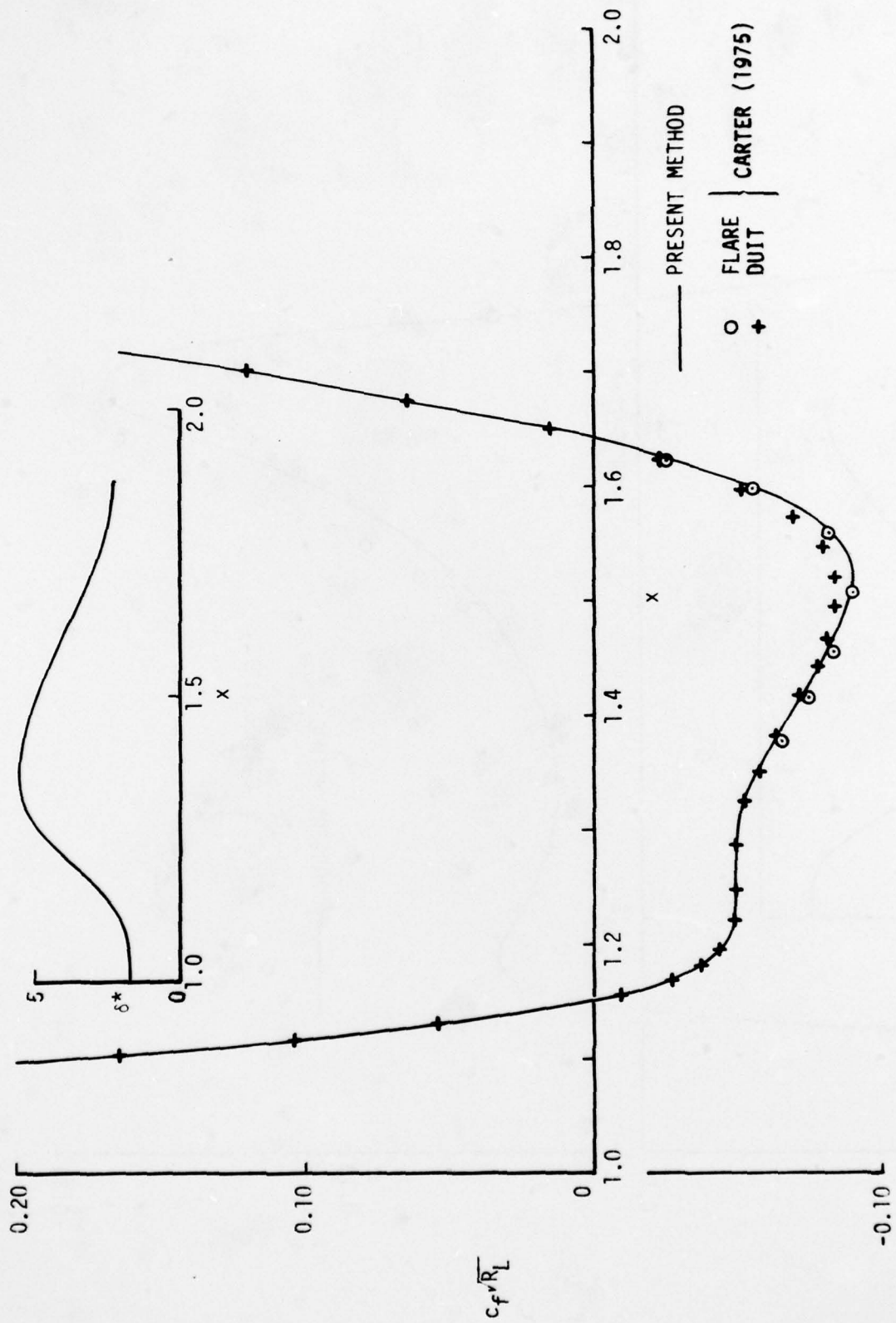


Figure 4. Local skin-friction distribution for Case A.

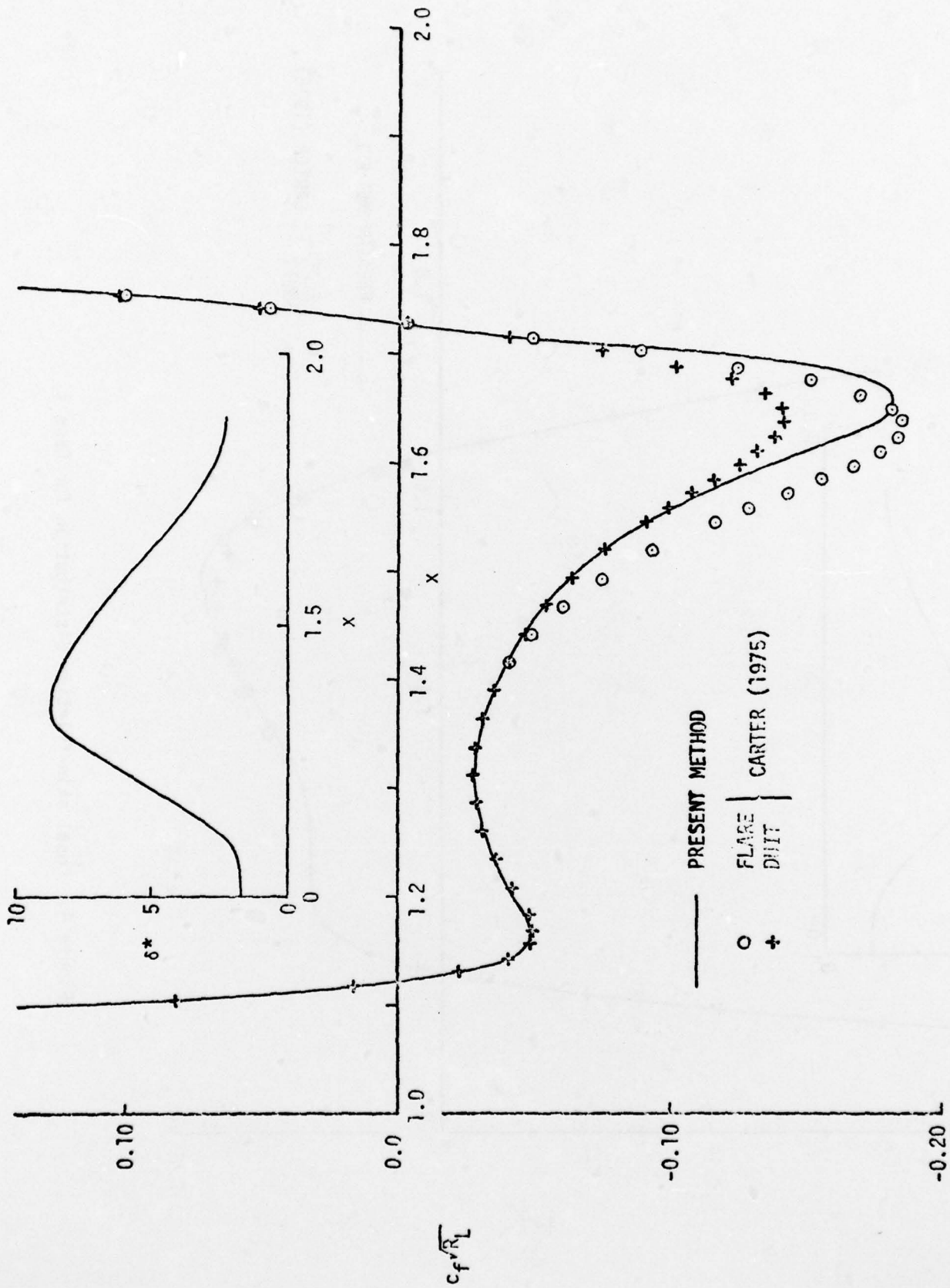


Figure 5. Local skin-friction distribution for Case B.

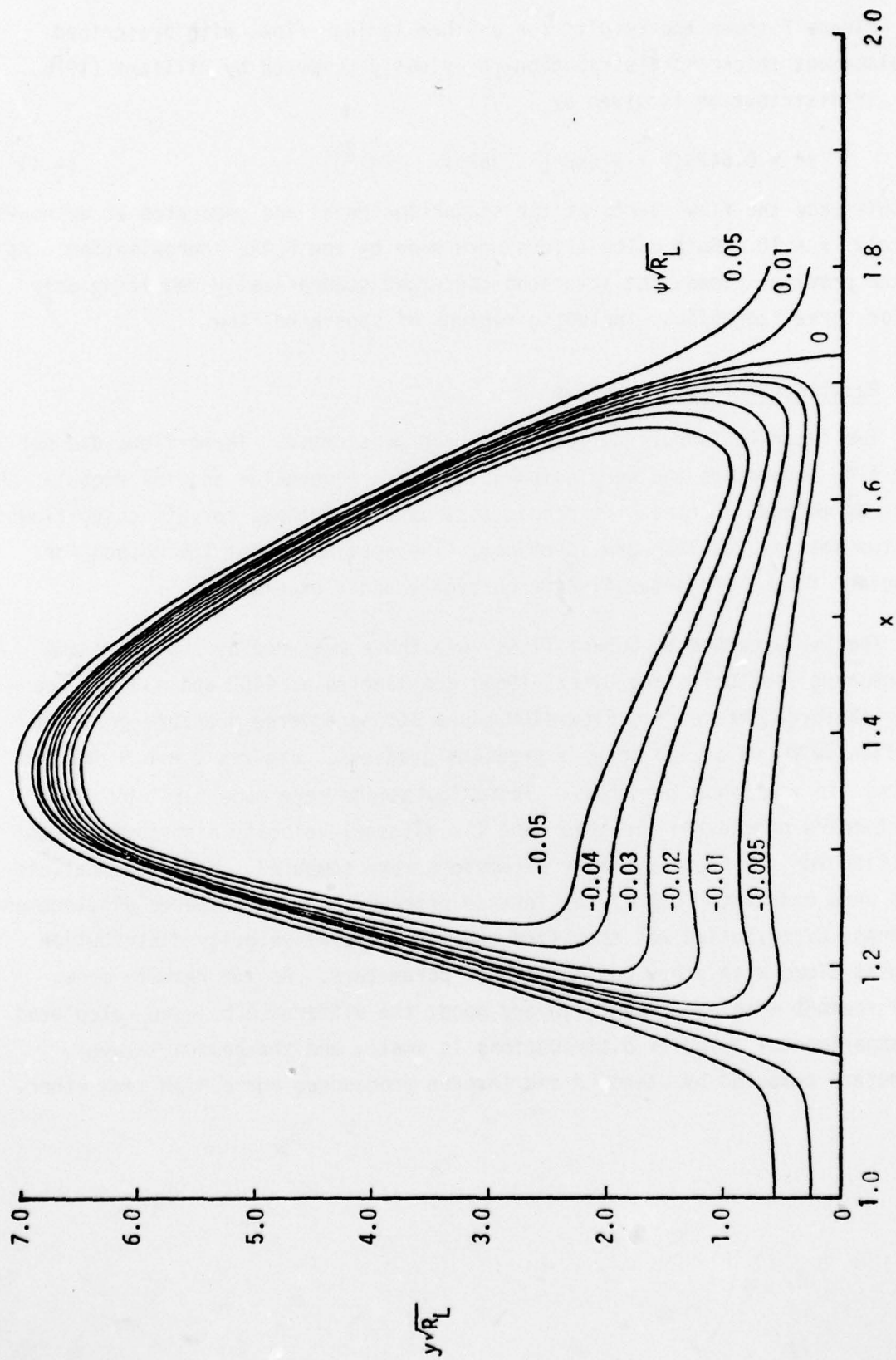


Figure 6. Streamline pattern in separation bubble for Case B.

Figure 7 shows the results for another laminar flow, with prescribed displacement thickness distribution, previously computed by Williams (1976). The  $\delta^*$ -distribution is given by

$$\delta^* = 0.6479\{1 + 9 \exp [-0.0625(x - 14)^2]\} \quad (4.4)$$

In this case the flow starts at the stagnation-point and separates at approximately  $x = 10$ . Both calculations were made by the FLARE approximation. As in the previous cases, the solutions converged quadratically requiring only two or three iterations, including regions of separated flow.

#### 4.2 Results for Turbulent Flows

Two separate turbulent flows have been considered. These flows did not have flow separation and were computed with the eigenvalue and the Mechul-function methods to check the predictions of both methods for attaching flows. The two sets of results were identical. The application of the method for turbulent flows with separation is currently under examination.

The two attached turbulent flows were those measured by Schubauer and Spangenberg (see Coles and Hirst, 1969) and labeled as 4400 and 4800 at the 1968 Stanford Conference. Flow 4400 has a strong adverse pressure gradient and flow 4800 has a mild adverse pressure gradient. Figures 8 and 9 present the results for these two flows. The calculations were made first by using the standard procedure: in this case the external velocity distribution was specified and the boundary-layer parameters were computed. Next, the calculations were made with both of the inverse procedures: the measured displacement thickness distribution was specified and the external velocity distribution computed along with other boundary-layer parameters. As the results show, the agreement with experiment is very good; the difference between calculated and experimental velocity distributions is small, and the boundary-layer parameters computed by standard and inverse procedures agree with each other.

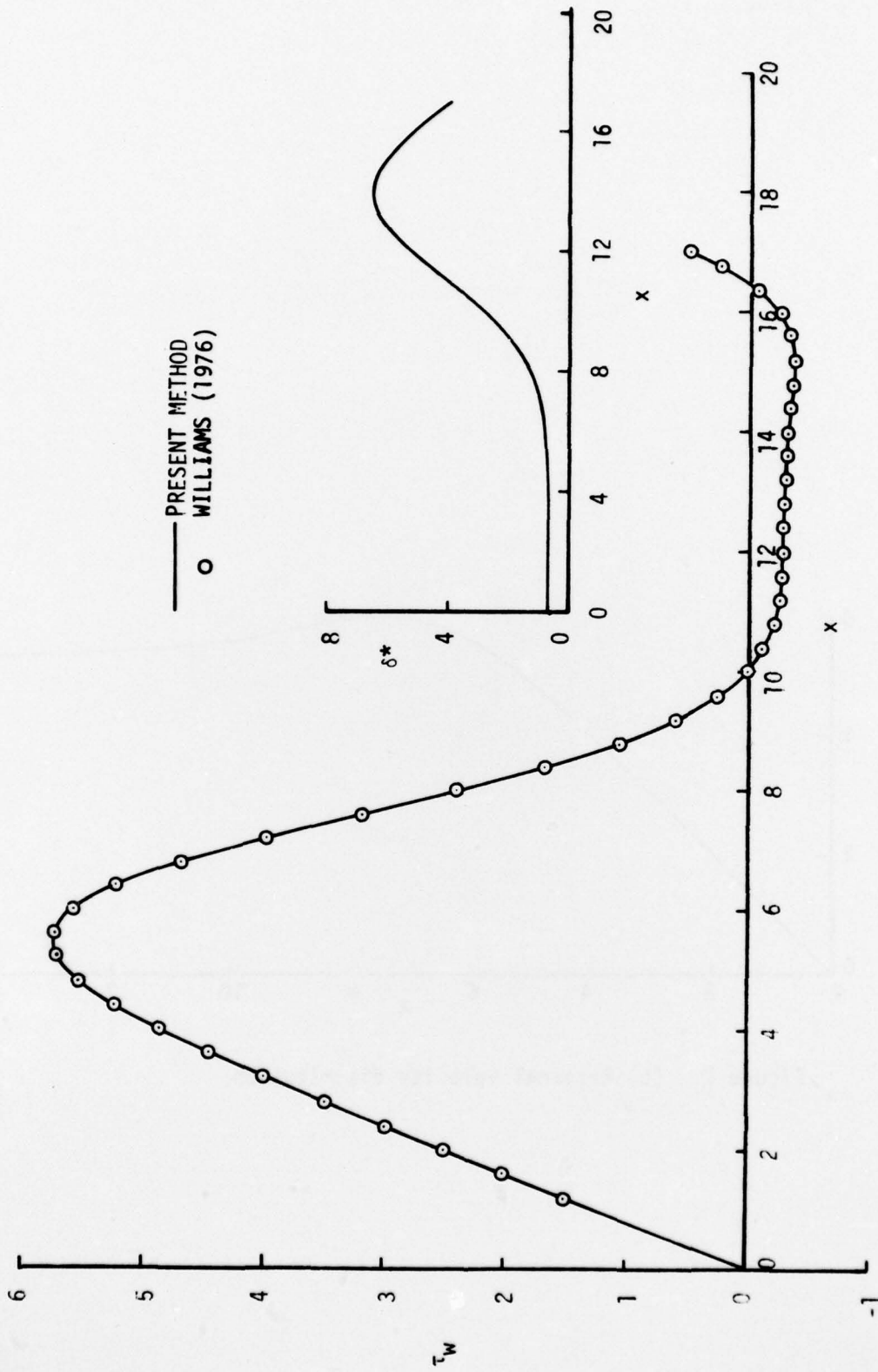


Figure 7. Comparison of calculated results for the separated flow for which displacement-thickness distribution is given by 4.4. (a) Wall shear distribution.

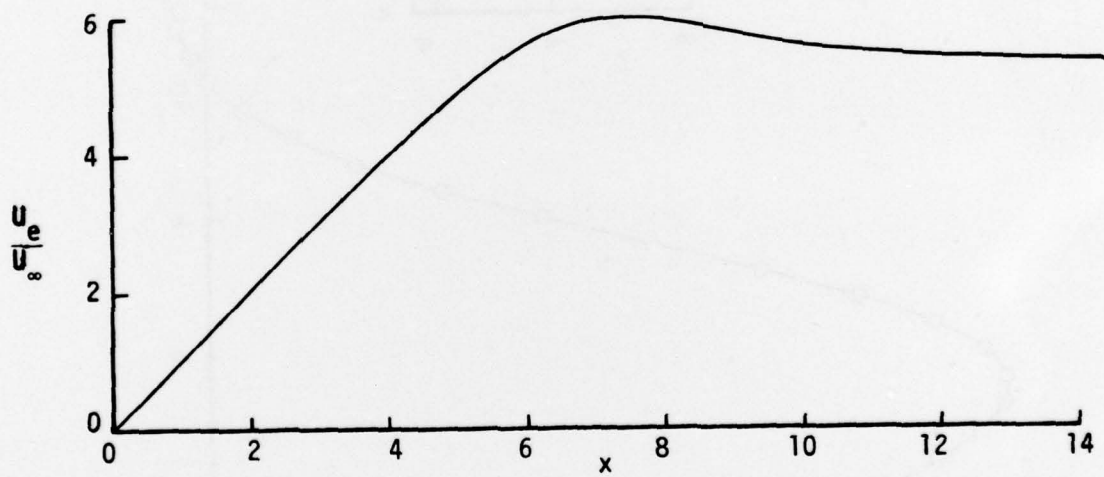


Figure 7. (b) External velocity distribution.

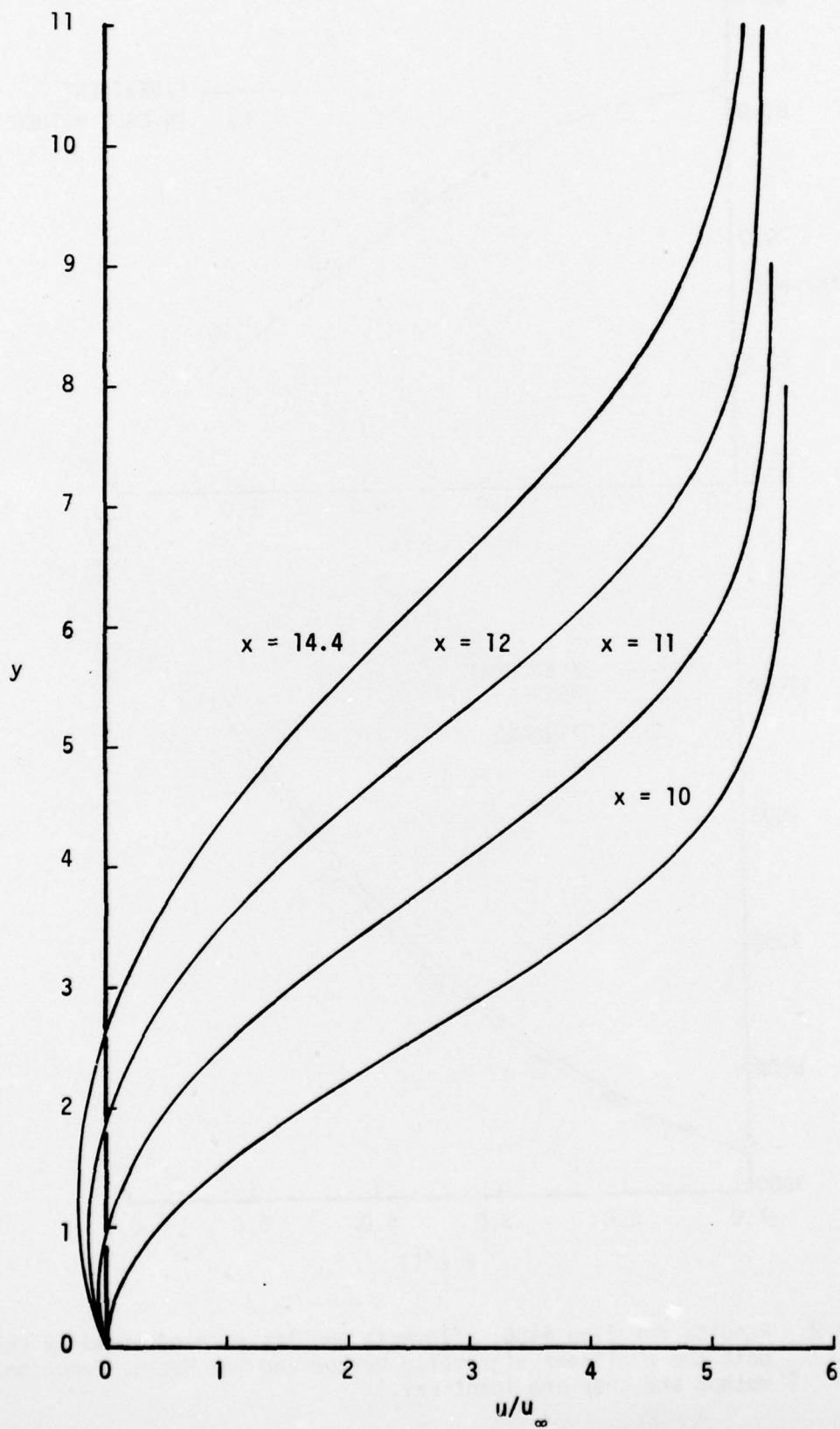


Figure 7. (c) Velocity profiles near and in the reverse flow region.

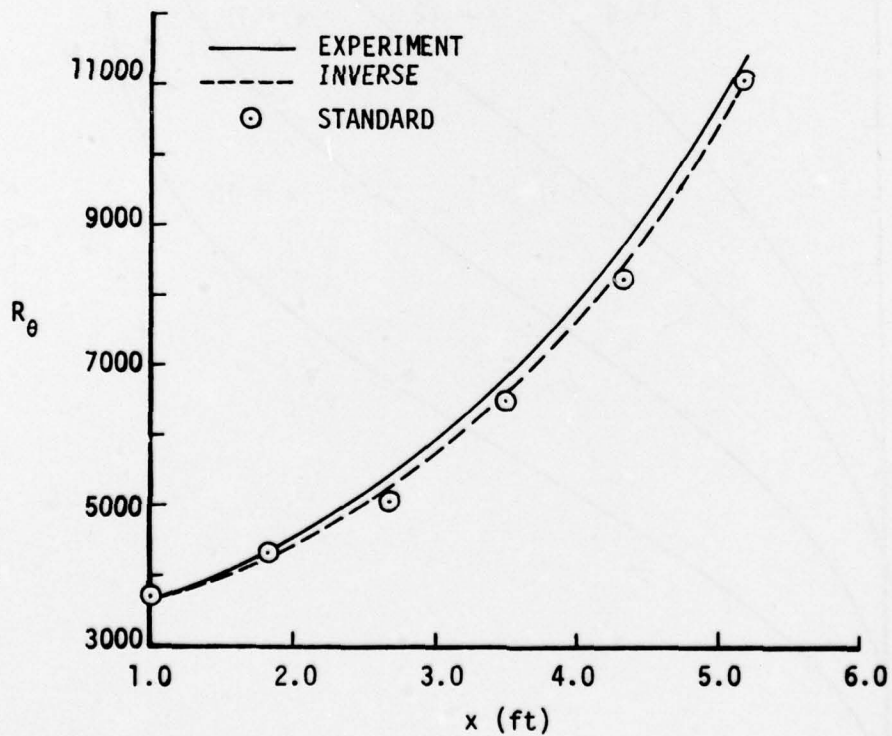
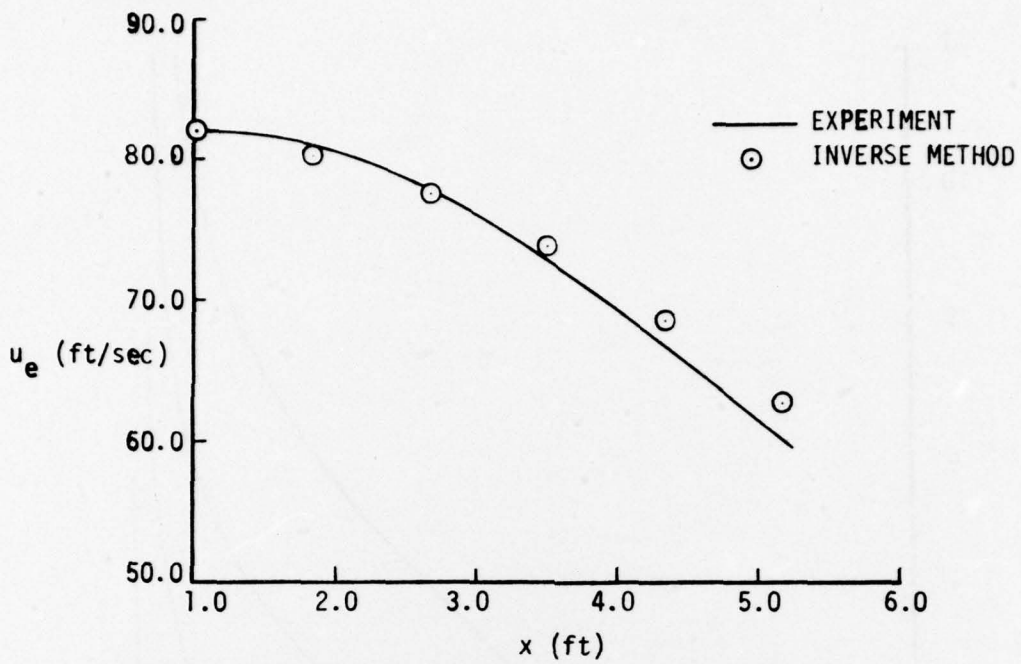


Figure 8. Results for flow 4400. (Inverse results were obtained by using both the nonlinear eigenvalue method and the Mechul-function method and they are identical.)

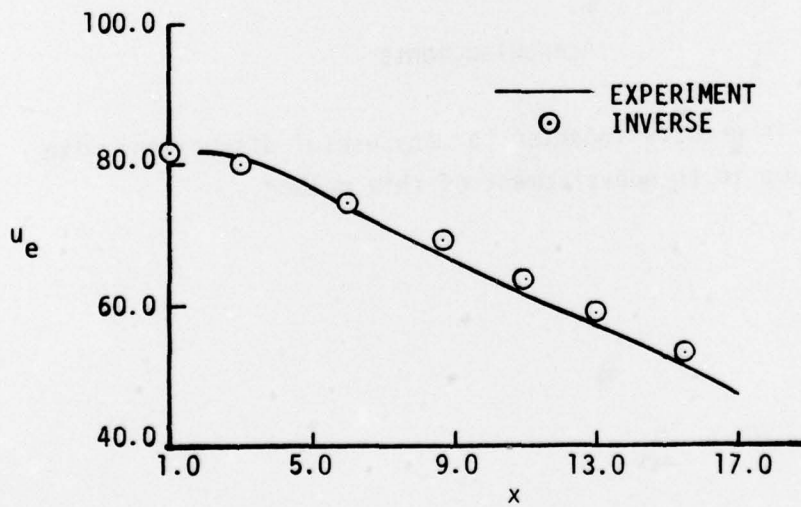
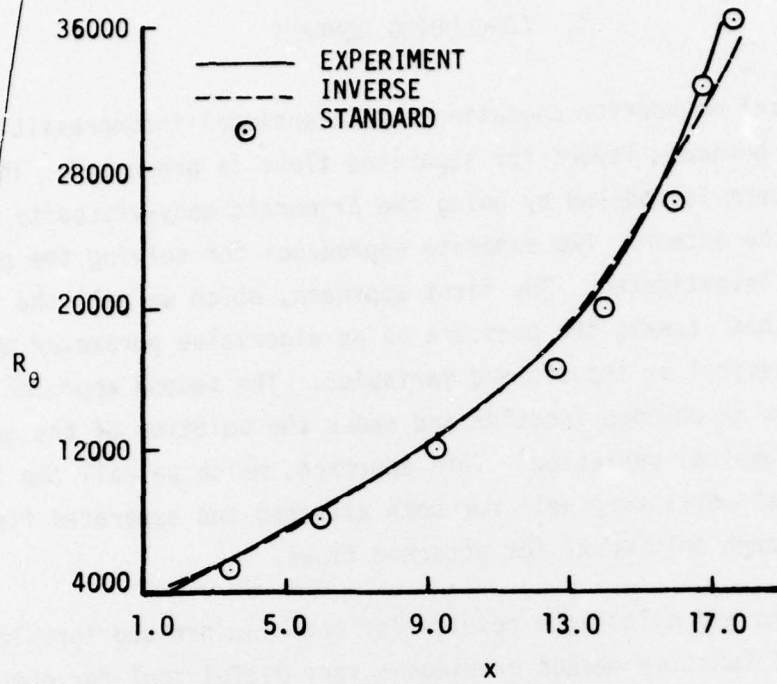


Figure 9. Results for flow 4800. (Inverse results were obtained by using both the nonlinear eigenvalue method and the Mechul-function method and they are identical.)

## 5. CONCLUDING REMARKS

A numerical method for computing two-dimensional incompressible laminar and turbulent boundary layers for separated flows is presented. The Reynolds shear stress term is modeled by using the algebraic eddy-viscosity formulas developed by the author. Two separate approaches for solving the governing equations are investigated. The first approach, which we call the "nonlinear eigenvalue method" treats the pressure as an eigenvalue parameter and works with either physical or transformed variables. The second approach treats the pressure as an unknown function and seeks the solution of the governing equations in physical variables. This approach, which we call the "Mechul function scheme" works very well for both attached and separated flows while the first approach only works for attached flows.

Comparisons and calculated results for both laminar and turbulent flows show the Mechul function method provides a very useful tool for computing the separated flows with the FLARE approximation. The computed results agree well with the available numerical and experimental results and show no signs of numerical problems in regions of negative wall shear.

### Acknowledgments

The author is greatly indebted to many useful discussions with Mr. P. G. Williams in the development of this method.

## 6. REFERENCES

- Briley, W.R. (1971) A Numerical Study of Laminar Separation Bubbles Using the Navier-Stokes Equations. *J. Fluid Mech.*, 47 (4) 713-736.
- Carter, J.E. (1974) Solutions for Laminar Boundary Layers with Separation and Reattachment. AIAA Paper No. 74-583.
- Carter, J.E. (1975) Inverse Solutions for Laminar Boundary-Layer Flows with Separation and Reattachment. NASA TR R-447.
- Carter, J.E. and Wornom, S.F. (1975) A Forward Marching Procedure for Separated Boundary-Layer Flows. *AIAA J.*, 13 (8) 1101-1103.
- Catherall, D. and Mangler, K.W. (1966) The Integration of the Two-Dimensional Laminar Boundary-Layer Equations Past the Point of Vanishing Skin Friction. *J. Fluid Mech.*, 26 (1) 163-182.
- Cebeci, T. (1974) Calculation of Three-Dimensional Boundary Layers. I. Swept Infinite Cylinders and Small Cross-Flow. *AIAA J.*, 12, 779-786.
- Cebeci, T. (1975a) An Inverse Boundary-Layer Method for Compressible Laminar and Turbulent Flows. Calif. State Univ. at Long Beach Rept. No. TR-75-1.
- Cebeci, T. (1975b) Calculation of Three-Dimensional Boundary Layers. II. Three-Dimensional Flows in Cartesian Coordinates. *AIAA J.*, 13, 1056-1064.
- Cebeci, T. and Bradshaw, P. (1977) Momentum Transfer in Boundary Layers. McGraw-Hill/Hemisphere, Washington D.C.
- Cebeci, T. and Smith, A.M.O. (1974) Analysis of Turbulent Boundary Layers. Academic Press, New York.
- Coles, D.E. and Hirst, E.A. (1969) Proceedings of Computation of Turbulent Boundary Layers, 1968 AFOSR-IFP-Stanford Conf., II. Thermosciences Div., Stanford Univ., Stanford Calif.
- Horton, H.P. (1974) Separating Laminar Boundary Layers with Prescribed Wall Shear. *AIAA J.*, 12 (12) 1772-1774.
- Isaacson, E. and Keller, H.B. (1966) Analysis of Numerical Methods. Wiley, New York.
- Keller, H.B. (1970) A New Difference Scheme for Parabolic Problems, in Numerical Solution of Partial Differential Equations (ed. J. Bramble), II, Academic Press, New York.

- Keller, H.B. and Cebeci, T. (1972) Accurate Numerical Methods for Boundary-Layer Flows. II. Two-Dimensional Turbulent Flows. AIAA J., 10 (9), 1193-1200.
- Klineberg, J.M. and Steger, J.L. (1974) On Laminar Boundary-Layer Separation. AIAA Paper No. 74-94, Jan/Feb.
- Kuhn, G.D. and Nielsen, J.N. (1973) Prediction of Turbulent Separated Boundary Layers. AIAA J., 12 (7) 881-882.
- Liebeck, R. H. (1976) On the Design of Subsonic Airfoils for High Lift. AIAA Paper No. 76-6463.
- Reyhner, T.A. and Flugge-Lotz, I. (1968) The Interaction of a Shock Wave with a Laminar Boundary Layer. Int. J. Non-Linear Mech., 3 (2) 173-199.
- Williams, P.G. (1975) A Reverse Flow Computation in the Theory of Self-Induced Separation. Proceedings of the Fourth International Conf. on Numerical Methods in Fluid Dynamics. Vol. 35 of Lecture Notes in Physics, Richtmyer, R.D. (ed), Springer-Verlag, 445-451.
- Williams, P.G. (1976) Private communication.

DISTRIBUTION LIST

Chief of Naval Research Department of the Navy Arlington, VA 22217 ATTN: Vehicles and Propulsion Program Code 211	5	Commandant of the Marine Corps Washington, DC 20380 ATTN: Dr. A. L. Slafkosky Scientific Advisor (Code RD-1)	1
Chief of Naval Development Department of the Navy Washington, DC 20360 ATTN: NAVMAT 0331 NAVMAT 0334	1 1	Defense Documentation Center Cameron Station, Bldg. 5 Alexandria, VA 22314	12
Naval Air Systems Command Department of the Navy Washington, DC 20361 ATTN: NAVAIR 320D NAVAIR 5301 NAVAIR 53013	1 1 1	Department of the Army DCS for Research and Development and Acquisition Washington, DC 20310 ATTN: DAMA-WSA (Mr. R. L. Ballard)	1
David Taylor Naval Ship Research & Development Center Bethesda, MD 20084 ATTN: Code 16 Code 522.3 Code 522.1	1 1 1	U. S. Army Material Command 5001 Eisenhower Avenue Alexandria, VA 22333 ATTN: AMCRD-F	1
Naval Research Laboratory Washington, DC 20375 ATTN: Technical Information Office, Code 2627 Library, Code 2629	1 1	Director, Headquarters U. S. Army Air Mobility R&D Lab. Ames Research Center Moffett Field, CA 94035	1
Superintendent U. S. Naval Academy Annapolis, MD 21402	1	Director, Ames Directorate U. S. Army Air Mobility R&D Lab. Ames Research Center Moffett Field, CA 94035	1
Superintendent U. S. Naval Postgraduate School Monterey, CA 93940	1	Director, Langley Directorate U. S. Army Air Mobility R&D Lab. Langley Research Center Hampton, VA 23665	1
Superintendent U. S. Naval Postgraduate School Monterey, CA 93940	1	Director, Eustis Directorate U. S. Army Air Mobility R&D Lab. Fort Eustis, VA 23604	1
U. S. Naval Air Development Center Warminster, PA 18974 ATTN: Aeromechanics Department	1	U. S. Air Force Flight Dynamics Laboratory Wright-Patterson AFB, OH 45433 ATTN: PT, Prototype Division FGC, Control Criteria Branch FXM, Aeromechanics Branch	1 1 1

Air Force Office of Scientific Research 1400 Wilson Boulevard Arlington, VA 22209 ATTN: Mechanics Division	1	ONR Branch Office Chicago 536 South Clark Street Chicago, IL 60605 ATTN: Mr. M. A. Chaszeyka	1
National Aeronautics and Space Administration 600 Independence Avenue, SW Washington, DC 20546 ATTN: Code RAA Code RAV	1 1	Lockheed Missiles & Space Co., Inc. Huntsville Research & Engineering Center P. O. Box 1103 Huntsville, AL 35807 ATTN: Mr. A. Zalay	1 1
National Aeronautics and Space Administration Ames Research Center Moffett Field, CA 94035 ATTN: Large-Scale Aerodynamics Branch	1	University of Cincinnati Department of Aerospace Engineering and Applied Mechanics Cincinnati, OH 45221 ATTN: Dr. R. T. Davis	1
National Aerodynamics and Space Administration Langley Research Center Hampton, VA 23665 Subsonic, Transonic Aerodynamics Division ATTN: Dr. James F. Campbell Dr. Stephen Wornom (Mail Stop 360)	1 1		
Commander, Air Force Plant Representative Office Lockheed-Georgia Company Marietta, GA 30068	1		
Office of Naval Research Department of the Navy Arlington, VA 22217 ATTN: Mr. M. Cooper, Code 430B	1		
ONR Branch Office 1030 East Green Street Pasadena, CA 91106 ATTN: Mr. B. F. Cagle	1		
Office of Naval Research Branch Office 495 Summer Street Boston, MA 02210 ATTN: Dr. A. D. Wood	1		